Since January 2020 Elsevier has created a COVID-19 resource centre with free information in English and Mandarin on the novel coronavirus COVID-19. The COVID-19 resource centre is hosted on Elsevier Connect, the company's public news and information website.

Vaccine 37 (2019) 5191–5202

Contents lists available at ScienceDirect

Vaccine

journal homepage: www.elsevier.com/locate/vaccine

Cricket paralysis virus internal ribosome entry site-derived RNA promotes conventional vaccine efficacy by enhancing a balanced Th1/Th2 response

Hye Won Kwak [a,1], Hyo-Jung Park [a,1], Hae Li Ko [a,1], Hyelim Park [a,1], Min Ho Cha [b,1], Sang-Myeong Lee [c,1], Kyung Won Kang [c,1], Rhoon-Ho Kim [a], Seung Rok Ryu [c], Hye-Jung Kim [a], Jae-Ouk Kim [d], Manki Song [d], Hun Kim [e], Dae Gwin Jeong [f], Eui-Cheol Shin [g], Jae-Hwan Nam [a,*]

[a] Department of Biotechnology, The Catholic University of Korea, Bucheon, Republic of Korea
[b] KM Application Center, Korea Institute of Oriental Medicine, Daegu, Republic of Korea
[c] Division of Biotechnology, The Chonbuk National University, Iksan, Republic of Korea
[d] Clinical Research Lab, International Vaccine Institute, Seoul National University Research Park, Seoul, Republic of Korea
[e] Life Science Research Institute, SK Bioscience, Seongnam, Republic of Korea
[f] Infectious Diseases Research Center, Korea Research Institute of Bioscience and Biotechnology, Daejeon, Republic of Korea
[g] Graduate School of Medical Science and Engineering, Korea Advanced Institute of Science and Technology, Daejeon, Republic of Korea

ARTICLE INFO

Article history:
Received 1 May 2019
Received in revised form 21 June 2019
Accepted 18 July 2019
Available online 29 July 2019

Keywords:
MERS
HPV
CrPV
IRES
RNA
Adjuvant
Vaccine
Th1/Th2
Alum

ABSTRACT

An ideal adjuvant should increase vaccine efficacy through balanced Th1/Th2 responses and be safe to use. Recombinant protein-based vaccines are usually formulated with aluminum (alum)-based adjuvants to ensure an adequate immune response. However, use of alum triggers a Th2-biased immune induction, and hence is not optimal. Although the adjuvanticity of RNA has been reported, a systematic and overall investigation on its efficacy is lacking. We found that single strand RNA (termed RNA adjuvant) derived from cricket paralysis virus intergenic region internal ribosome entry site induced the expression of various adjuvant-function-related genes, such as type 1 and 2 interferon (IFN) and toll-like receptor (TLR), T cell activation, and leukocyte chemotaxis in human peripheral blood mononuclear cells; furthermore, its innate and IFN transcriptome profile patterns were similar to those of a live-attenuated yellow fever vaccine. This suggests that protein-based vaccines formulated using RNA adjuvant function as live-attenuated vaccines. Application of the RNA adjuvant in mouse enhanced the efficacy of Middle East respiratory syndrome spike protein, a protein-subunit vaccine and human papillomavirus L1 protein, a virus-like particle vaccine, by activating innate immune response through TLR7 and enhancing pAPC chemotaxis, leading to a balanced Th1/Th2 responses. Moreover, the combination of alum and the RNA adjuvant synergistically induced humoral and cellular immune responses and endowed long-term immunity. Therefore, RNA adjuvants have broad applicability and can be used with all conventional vaccines to improve vaccine efficacy qualitatively and quantitively.

1. Introduction

Although inactivated and protein-based vaccines have long been used to prevent the spread of various pathogens [1] successfully, some of them elicit a weak immune response, short immune duration, and have several safety issues [2,3]. Therefore, research has focused on identifying antigen components responsible for immunogenicity in order to generate safer and more effective vaccines. However, purified recombinant antigens generally show poor immunogenicity [2]. To overcome this, immunostimulatory agents (i.e., adjuvants) are added to vaccines to induce robust immune responses against vaccine antigens [4–6].

Abbreviations: APCs, Antigen presenting cells; DCs, dendritic cells; Th2, T helper 2; TLR, Toll-like receptor; IFN, interferon; ssRNAs, single-stranded RNAs; IL, interleukin; Tfh, follicular helper T; RIG, retinoic acid-inducible gene; IRESs, internal ribosome entry sites; CrPV, Cricket paralysis virus; IGR, intergenic region; MERS, Middle East respiratory syndrome; CoV, coronavirus; HPV, human papillomavirus; dLN, draining lymph node; NAbs, neutralizing antibodies; VLP, virus-like particle; Tg, transgenic; WT, wild-type; ELISA, enzyme-linked immunosorbent assay; PRNT, plaque-reduction neutralization test; PFUs, plaque-forming units; ELISPOT, enzyme-linked immunospot; hPBMCs, human peripheral blood mononuclear cells; TNF, tumor necrosis factor; Myd88, myeloid differentiation primary response 88.

* Corresponding author at: Department of Biotechnology, The Catholic University of Korea, 43-1, Bucheon, Gyeonggi-do 14662, Republic of Korea.
E-mail address: jhnam@catholic.ac.kr (J.-H. Nam).
[1] These authors contributed equally to this work.

https://doi.org/10.1016/j.vaccine.2019.07.070
0264-410X/

Aluminum hydroxide (alum) is widely used as an adjuvant in several human vaccines [7]. It has been reported that alum injection leads to the rapid accumulation of neutrophils and other cells forming lumps composed of neutrophil extracellular traps. This further induces lysosome-mediated lysis to distort the plasma membrane of antigen presenting cells (APCs) and/or rapidly induces the synthesis cytokines/chemokines, finally activating the NALP3 inflammasome and triggering the secretion of IL-1β. This process might contribute to the adjuvant effect of alum. However, further confirmation is required [8]. In addition, alum induces a profound T helper 2 (Th2) response along with antibody production. However, alum cannot induce Th1 responses and sometimes stimulates autoimmunity by upregulating IgE presentation [9]. Since classical adjuvants solely induce Th2 responses, new adjuvants capable of promoting Th1 responses are required to increase the cell-mediated response [8]. Non-classical adjuvants, such as Toll-like receptor (TLR) ligands, can stimulate the production of type I interferon (IFN) and proinflammatory cytokines [10]. Type I IFN facilitates antigen presentation to major histocompatibility complex class I/II, leading to an enhanced cytotoxic CD8+ T cell response, as well as a CD4+ T cell response [11].

Since its first use as an adjuvant with the inactivated Japanese encephalitis virus (JEV) vaccine to efficiently promote neutralizing antibodies (NAbs), IFN production, and resistance to JEV infection, poly I:C and its derivates have been widely used in the development of various vaccines [12,13]. In addition, RNase-resistant poly I:C stabilized with poly-L-lysine (poly ICLC) was shown to have strong adjuvanticity by microbial mimicking for inducing innate immune responses in humans through TLR3 and MDA5 [14]. Despite the strong adjuvanticity of poly I:C, there are concerns about its induction of adverse and excessive immune responses, such as autoimmune diseases and difficulty in standardization for mass production [15]. In previous studies, poly I:C-induced massive type I IFNs were shown to be critical for the pathogenesis of lupus [16]. Moreover, repeated administration of poly I:C derivate, poly ICLC, and carboxymethylcellulose, showed severe pathogenicity and resulted in the development of tuberculosis in mice [17].

Single-stranded RNAs (ssRNAs) function as vaccine adjuvants and promote Th1 responses through the induction of IFN-α and interleukin (IL)-12 in DCs [18]. Sendai virus-derived defective interfering RNA activates the innate immune response, leading to increased efficacy of inactivated influenza vaccine [19]. Additionally, nucleoside-modified influenza mRNA vaccines showed adjuvant effects by inducing antigen-specific follicular helper T (Tfh) cells and germinal center B cell responses [20]. Recently, ssRNA formulated with carriers showed immune-enhancement effects through TLR and retinoic acid-inducible gene (RIG)-like helicase signaling pathways [21,22]. Although these studies demonstrated that ssRNAs could function as adjuvants, systematic investigations of their effects and applicability to protein-based or inactivated vaccines are lacking, thereby preventing their widespread clinical adoption.

We previously developed novel ssRNA-expression platforms from several viral internal ribosome entry sites (IRESs) [23]. In this study, we investigated the adjuvant effects of ssRNAs (RNA adjuvant) derived from the Cricket paralysis virus (CrPV) intergenic region (IGR) IRES [23]. We formulated the RNA adjuvant with protein-subunit vaccine for Middle East Respiratory Syndrome (MERS)-coronavirus (CoV) and virus-like particle vaccine for human papillomavirus (HPV) and showed that the RNA adjuvant induced a balanced Th1/Th2 response and innate immunity. Moreover, as expected, the RNA adjuvant worked through TLR7 and recruited APCs to increase antigen uptake into the injected site and their retention in the draining lymph node (dLN). Furthermore, we showed that the RNA adjuvant enhanced humoral and cellular immune responses by promoting antigen-specific neutralizing antibodies (NAbs) and the Th1 response and ultimately endowing long-term immunity. The results demonstrated that an RNA adjuvant could be developed as a general, safe, and effective adjuvant applicable to protein-based vaccine types.

2. Material and methods

2.1. Mice

For immunization with MERS S soluble protein vaccine and HPV L1 virus-like particle (VLP) vaccine, female BALB/c and C57BL/6 mice were purchased from Dae-Han Bio-Link. Female TLR7 KO mice were kindly provided by Dr. Bumseok Kim, Chonbuk National University, and hDPP4 Tg mice, stably expressing hDPP4 as the MERS-CoV receptor, were kindly provided by Dr. Sungkyun Park, Korea Research Institute of Bioscience & Biotechnology. Mice were housed at the Catholic University of Korea under specific-pathogen-free conditions with 12-h light/dark cycle and handled according to protocols approved by the Catholic University of Korea. The animal facility at the Catholic University of Korea is fully accredited by the Korean Association for Laboratory Animals. All mice experimental procedures conducted in this study followed the guidelines of the Institutional Animal Care and Use Committee of the Catholic University of Korea (*CUK-IACUC-2016-039, 2016-046, 2017-028, 2018-027,* and *2018-028*).

For MERS-CoV challenge, hDPP4-transgenic (Tg) mice (5–7-weeks old) were maintained in a biosafety level 3 facility at the Korea Zoonosis Research Institute of Chonbuk National University and followed the guidelines of the Institutional Animal Care and Use Committee (*2018-045*).

2.2. Vaccines

Soluble MERS spike (S) protein vaccine was provided by the International Vaccine Institute (Seoul, Korea). This MERS S protein expressed in insect cells has no transmembrane domain and comprises the first 1296 amino acids of MERS-CoV EMC/2012 strain (GenBank #AFS88936.1). VLPs containing HPV L1 (a mixture of 10 types of L1 – 6, 11, 16, 18, 31, 33, 35, 45, 52, and 58 L1) were obtained from SK Bioscience (Seoul, Korea) and expressed in insect cells. Due to patent issues, detailed information on the HPV vaccine was unavailable.

2.3. In vitro transcription and RNA purification

The DNA platform was designed using the IGR IRES and SV40 late-polyadenylation signal sequences (Supplementary Fig. 1) [23]. DNA templates were linearized with *Not*I. *In vitro* transcription was performed using the EZ T7 high yield *in vitro* transcription kit (Enzynomics, Daejeon, Korea) and HiScribe T7 Quick high yield RNA synthesis kit (New England Biolabs, Ipswich, MA, USA). See Supplementary Methods for more details.

2.4. Analysis of transcriptome in human PBMC

Human peripheral blood mononuclear cells (hPBMCs) obtained from Zen bio were cultured in RPMI 1640 medium (Hyclone Laboratories Inc, South Logan, UT, USA) supplemented with 10% heat-inactivated FBS (Life Technologies, Carlsbad, CA, USA), 2.05 mM L-glutamine (Hyclone Laboratories Inc, South Logan, UT, USA), and 1% Pen-Strep Glutamine (Gibco, Waltham, MA, USA). Cells were maintained in a humidified atmosphere at 37 °C with 5% CO_2. PBMCs were stimulated with 10 μg/ml of poly I:C (Sigma

Aldrich, St. Louis, MO, USA) and 20 μg/ml of RNA adjuvant for 6 and 24 h. See Supplementary Methods for more details.

2.5. Immunization

For MERS S protein vaccine studies, C57BL/6 WT and hDPP4-Tg mice (6-weeks old) were inoculated intramuscularly into the upper thigh twice a week at 2-week intervals with the following formulations: (1) 1 μg MERS S protein vaccine with/without 20 μg RNA adjuvant or 500 μg alum (Thermo Fisher Scientific, Waltham, MA, USA) for wild-type (WT) mice; and (2) 1 μg MERS S protein vaccine with/without 20 μg RNA adjuvant or 24 μg alum (Brentanne, Frederikssund, Denmark) for hDPP4-Tg mice. For VLP-HPV-L1 vaccine studies, BALB/c mice (6-weeks old) were inoculated by intramuscular injection into the upper thigh three times a week at 2-week intervals with 6 μg VLP-HPV-L1 with/without 20 μg protamine-formulated RNA adjuvant or 5 μg alum.

2.6. Enzyme-linked immunosorbent assay (ELISA)

Antigen-specific IgG1, IgG2a, and IgG2c in mouse serum were measured by ELISA. The 96-well plates (Corning, Corning, YN, USA) were coated with 50 ng/well MERS S protein and 100 ng/well VLP-HPV-L1 vaccine and incubated overnight at 4 °C. See Supplementary Methods for more details.

2.7. Plaque-reduction neutralization test (PRNT) for MERS-CoV and HPV

Serum from MERS-CoV infected hDPP4-Tg mice were serially diluted from 10- to 5120-fold with serum-free medium, and the virus-serum mixture was prepared by mixing 100 plaque-forming units (PFUs) of MERS-CoV using the diluted serum samples and incubated at 37 °C for 1-h. HPV-specific NAb titration was performed as described previously [24]. See Supplementary Methods for more details.

2.8. Enzyme-linked immunospot (ELISPOT)

Splenocytes from immunized mice and GPs at the end of the experiments were stimulated with 0.125–1 μg/well of antigens for 48 h at 37 °C. ELISPOT for the detection of IFN-γ-secreting T cells was performed according to manufacturer instructions (Mabtech, Stockholm, Sweden).

2.9. Flow cytometry

For surface staining, splenocytes and isolated immune cells from muscle and lymph nodes were stained with the following antibodies for 15 min at room temperature; CD4 (Clone GK1.5, eBioscience; Clone H129.19, Bio Legend), CD8 (Clone 53-6.7, BD Biosciences; Clone 53-6.7, Invitrogen), CD69 (Clone H1.2F3, BD Biosciences), CD44 (Clone IM7, Invitrogen), CD62L (Clone MEL 14, BD Biosciences), CD11b (Clone M1/70, Bio Legend), F4/80 (Clone BM8, Invitrogen), CD86 (Clone GL1, BD Biosciences), and CD11c (Clone N48, eBioscience). Cells were fixed with 1% paraformaldehyde, analyzed using a FACS Canto II flow cytometer (BD Biosciences), and the data were analyzed using FlowJo (TreeStar). For determining polyfunctional T cells, isolated splenocytes were re-stimulated with 1 μg/well MERS spike protein or 100 ng/well of the peptide mixture. To evaluate the cytotoxic degranulation activity of T cells, anti-CD107a-BV421 (Clone 1D4B, BD Biosciences) was added into the culture medium. Brefeldin A (GolgiPlug, BD Biosciences) and monensin (GolgiStop, BD Biosciences) were added 2 h later. After another 10 h incubation, splenocytes were first stained with ethidium monoazide (Sigma) and then stained with anti-CD3-BV510, anti-CD4-APCH7, and anti-CD8-PE-cy7 (Clone 145-2C11, Clone GK1.5, and Clone 53-6.7) (BD Biosciences). The stained cells were permeabilized using Cytofix/Cytoperm kit (eBioscience) and then stained with anti-IFN-γ-APC, anti-TNF-α-FITC, and anti-IL-2-PE (Clone XMG1.2, BD Biosciences; Clone MP6-XT22, Invitrogen; Clone JES6-5H4, eBioscience). Cells were fixed with 1% paraformaldehyde, analyzed using an LSRII flow cytometer (BD Biosciences), and T cells positive for the various combinations of cytokines and degranulation were analyzed and quantified using a Boolean gating function in FlowJo (TreeStar).

2.10. In vivo imaging and image processing

A laser-scanning intravital confocal microscope (IVM-C, IVIM Technology) was used to visualize dendritic cells and monocyte recruitment. CX3CR1-GFP mice (Jackson Laboratory, Bar Harbor, ME, USA, stock #005582) that endogenously express GFP in dendritic cells and monocytes were used. Mice were deeply anesthetized with intraperitoneal injections of zoletil (30 mg/kg) and rompun (10 mg/kg). During imaging, mouse body temperature was maintained at 37 °C with a homeothermic controller (PhysioSuite; RightTemp; Kent Scientific). A mixture of Alexa Fluor 647 (A20006, Thermo Fisher Scientific) and either RNA adjuvant or PBS was subcutaneously injected into the mouse ear skin using a 31G microinjector (1700 series syringe, Hamilton). To label vasculatures, an anti-CD31 antibody (553369, BD Biosciences) conjugated with Alexa Flour 555 (A20009, Thermo Fisher Scientific) was injected intravascularly 1 h before imaging. Using the distinctive vasculature and the fluorescence signal of Alexa Fluor 647 as a landmark for the repetitive imaging of the injected site, the recruitment of CX3CR1-GFP$^+$ dendritic cells (irregular outlines) and monocytes (round outlines) was imaged *in vivo* at 20 min and 24 h after the injection. The recruitment of dendritic cells and monocytes was quantified by calculating the area occupied by CX3CR1-GFP$^+$ cells using ImageJ plugins (NIH).

2.11. Multiplex cytokine assay

After stimulating the human peripheral blood mononuclear cells (hPBMCs) with the RNA adjuvant for 24 h, concentrations of tumor necrosis factor (TNF)-α, IFN-γ, IL-2, IL-12, IL-6, and IL-10 were analyzed using the Magnetic Luminex screening assay kit (R&D Systems, Minneapolis, MN, USA) according to manufacturer instructions.

2.12. Depletion of CD4+ and/or CD8+ T cells

To examine the effects on T cells, C57BL/6 mice (6-weeks old) were inoculated by intramuscular injection twice at 6-day intervals with 1 μg MERS S protein vaccine with 20 μg RNA adjuvant, followed by inoculation by intraperitoneal injection with 10 mg/kg anti-mouse CD4 (YTS 191; BioXcell, West Lebanon, NH, USA) and/or 10 mg/kg anti-mouse CD8 (YTS 169.4; BioXcell) every 3-days after the first immunization.

2.13. Statistical analyses

One-way analysis of variance was used to assess significant differences among treatment groups. For each significant treatment effect, the Tukey HSD test was used to compare multiple group means. In addition, all histomorphometrical values are expressed as means ± standard deviation (SD). Multiple comparison tests for the different treatment groups were conducted. If the Levene test indicated no significant deviations from variance homogeneity, the data obtained were analyzed by a least-significant differences

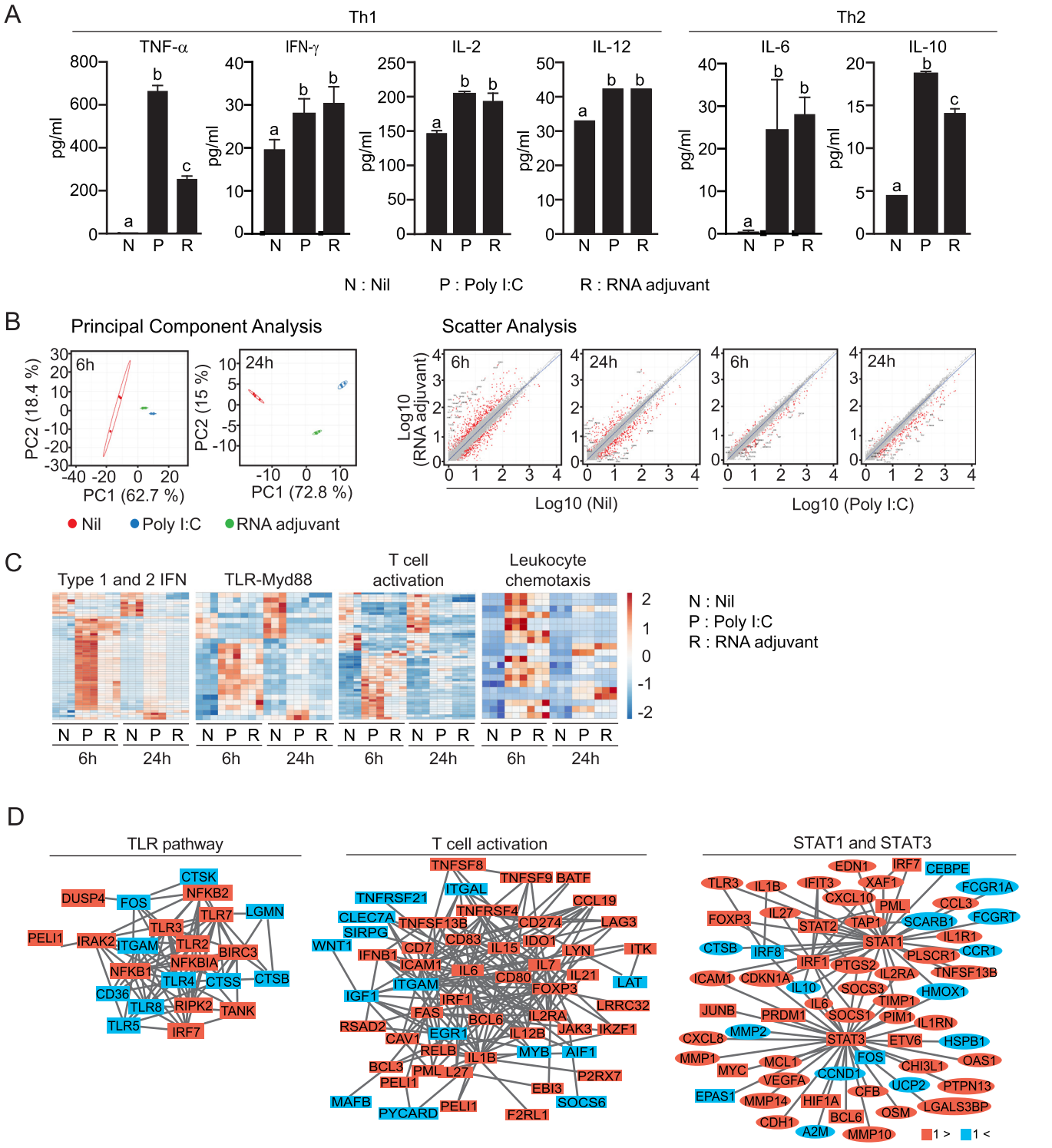

Fig. 1. The RNA adjuvant induces transcriptional profiles similar to those induced by poly(I:C) in hPBMCs. hPBMCs were stimulated with RNA adjuvant or poly(I:C) for 6-h and 24-h. Nil indicates PBS treatment. (*A*) Th1- and Th2-related cytokine production in the hPBMC supernatant was measured by multiplex analyses at 24-h post-stimulation. The data were statistically analyzed by ANOVA. The significance of differences between groups is indicated by different letters of the alphabet. $p < 0.05$. Data are presented as mean ± standard deviation ($n = 3$). (*B*) Principal component analysis plots for all samples (three samples per group at 6- and 24-h post-treatment) (left) and scatter plots (right) of RNA-seq data (fold ratio ≥ 0.7). Nil indicates PBS-treated hPBMCs. (*C*) Heat maps showing clustering based on the signaling pathways associated with type 1 and 2 IFNs, TLR-Myd88), T cell activation, and leukocyte chemotaxis. (*D*) Simulated dynamics of the transcriptional network representing differentially expressed genes (DEGs). Interaction of proteins involved in the TLR signaling pathway, T cell activation, and proteins interacting with STAT1 and STAT3 (each square indicates a transcriptional factor, and each circle indicates a gene affected by a transcriptional factor). Red nodes are upregulated, and blue nodes are downregulated DEGs (fold-change ratio > 1). DEGs: differentially expressed genes, TLR: Toll-like receptor, Myd-88: myeloid differentiation primary response 88, Th: T helper cell, PBS: phosphate-buffered saline, hPBMC: human peripheral blood mononuclear cells, STAT: signal transducer and activator of transcription. (For interpretation of the references to color in this figure legend, the reader is referred to the web version of this article.)

multi-comparison test. If significant deviations from variance homogeneity were detected using the Levene test, the non-parametric Kruskal–Wallis H-test was conducted. When a significant difference was detected by the Kruskal–Wallis H-test, a Mann–Whitney U-test was conducted as a post hoc analysis. Statistical analyses were conducted using SPSS for Windows (Release 14.0K, SPSS Inc.). To assess significant differences between two groups, Student's *t*-test was used. Differences were considered significant at $P < 0.05$.

3. Results

3.1. The RNA adjuvant affects genes related to the innate immune responses, T cell activation, and chemotaxis similar to poly(I:C) in hPBMCs

To investigate the adjuvant effect, we treated hPBMCs with the RNA adjuvant and used poly(I:C) as a positive control, finding that the RNA adjuvant induced Th1- and Th2-related cytokine release similar to poly(I:C) (Fig. 1A). We then compared the transcriptome profiles of RNA adjuvant- and poly(I:C)-treated hPBMCs by RNA sequencing. Control, poly(I:C), and RNA adjuvant treatment formed a separate cluster without any bias (Fig. 1B), with scatter plots of gene profiling confirming that changes in gene-expression between the RNA adjuvant and poly(I:C) groups were not greater than those between the control and RNA adjuvant groups at 6- and 24-h post-treatment ($p \leq 0.05$; fold-change ≥ 2) (Fig. 1B).

To investigate the biological pathways associated with genes affected by the RNA adjuvant, we analyzed gene-expression patterns using the Kyoto Encyclopedia of Genes and Genomes database (https://www.genome.jp/kegg/mapper.html) (Fig. 1C) and the network of genes involved in each pathway based on the STRING database (Fig. 1D). After 6-h, similar biological pathways were affected by RNA adjuvant and poly(I:C) treatment (Supplementary Fig. 2), and heat maps of innate-immune-related genes [type 1 and 2 IFNs and TLR-myeloid differentiation primary response 88 (Myd88)], as well as T cell activation and leukocyte chemotaxis, indicated similar expression patterns between the two groups (Fig. 1C). *TLR2, TLR3, TLR7*, *IRF7,* and *NF-κB* among the TLR related genes were induced, and *IL-6* and *IL-15* among T cell activation related genes and *STAT 1* and *3* among multiple transcriptional factors function as key players in the RNA adjuvant group (Fig. 1D).

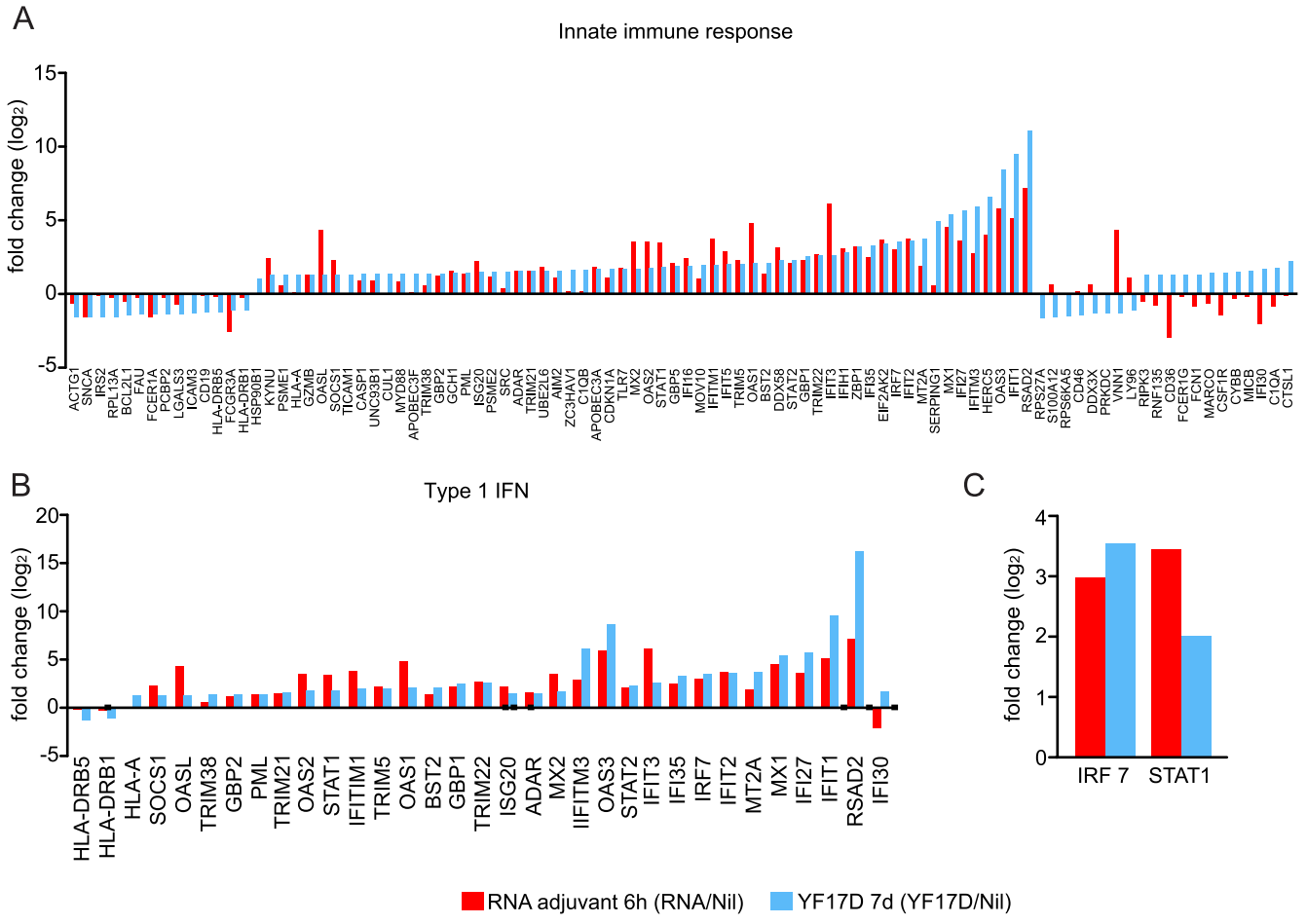

Fig. 2. The RNA adjuvant mimics live-attenuated vaccine YF17D in transcription profiles associated with the innate immune response. Transcription profiles in response to live-attenuated vaccine YF17D in hPBMCs isolated from an immunized patient 7-days after vaccination (fold-change ≥ 2; $p < 0.05$; $n = 30$) and in response to the RNA adjuvant from hPBMCs at 6-h post-treatment. Induction and reduction profiles of genes related to innate immune responses (*A*) and type 1 IFN (*B*) from the RNA adjuvant (red) and YF17D (blue). (*C*) Comparison of *IRF7* and *STAT1* induction between RNA adjuvant (red) and YF17D (blue) treatment. Fold-change (log2) in expression in response treatment indicating the change in expression of each gene at 6-h post-treatment with the RNA adjuvant as compared PBS (RNA/Nil) and at 7-days post-immunization with YF17D as compared with that before immunization (YF17D/Nil). PBS: phosphate-buffered saline, hPBMC: human peripheral blood mononuclear cells, STAT: signal transducer and activator of transcription, IRF: interferon regulatory factor. (For interpretation of the references to color in this figure legend, the reader is referred to the web version of this article.)

3.2. The RNA adjuvant induces a transcriptional profile similar to that by a live-attenuated vaccine

Yellow fever vaccine (YF17D) is the most successful live-attenuated vaccine, as its duration of protective immunity after single immunization is >35 years [25]. We compared the transcription profile induced in RNA adjuvant-treated hPBMCs (6-h post-treatment) with that of PBMCs obtained from a YF17D-immunized patient (at 7-days post-immunization) [26]. Approximately 80% of the innate immune response and 100% of type I IFN-related genes, which are key factors contributing to a superior vaccine [14,27], showed similar changes in expression pattern between the two samples (Fig. 2A and B). The inductions of *IRF7* and *STAT1* are important upstream immune transcription factors targeting different effectors of the immune response to the YF17D vaccine [26]. Interestingly, increases in *IRF7* and *STAT1* levels in response to the RNA adjuvant were the same as those in response to YF17D (Fig. 2C), indicating that the RNA adjuvant affected important transcription factors that play key roles in YF17D-vaccine efficacy.

3.3. The RNA adjuvant recruits APCs to the injection site and increases their retention in the dLN

The RNA adjuvant increased APC retention in the dLN to promote selection of antigen-specific T and B cells by epitope-presenting APCs in a process similar to that observed following treatment with poly(I:C) (Fig. 3A). Furthermore, *in vivo* time-lapse imaging clearly showed that the RNA adjuvant summoned immune cells, mostly DCs (irregular outlines), to the injection site (Fig. 3B and C), which was consistent with the heat map describing upregulated leukocyte chemotaxis (Fig. 1C) and indicating that the RNA adjuvant enhanced antigen uptake by DCs at injection sites and promoted epitope presentation in the dLN.

3.4. The RNA adjuvant activates the Th1 response, synergistically increases the level of NAbs, and protects against MERS-CoV challenge

To confirm adjuvant effects *in vivo*, we formulated it with the MERS spike (S) protein and used it to immunize WT C57BL/6 mice with/without alum (Fig. 4A). At 2-weeks after first immunization,

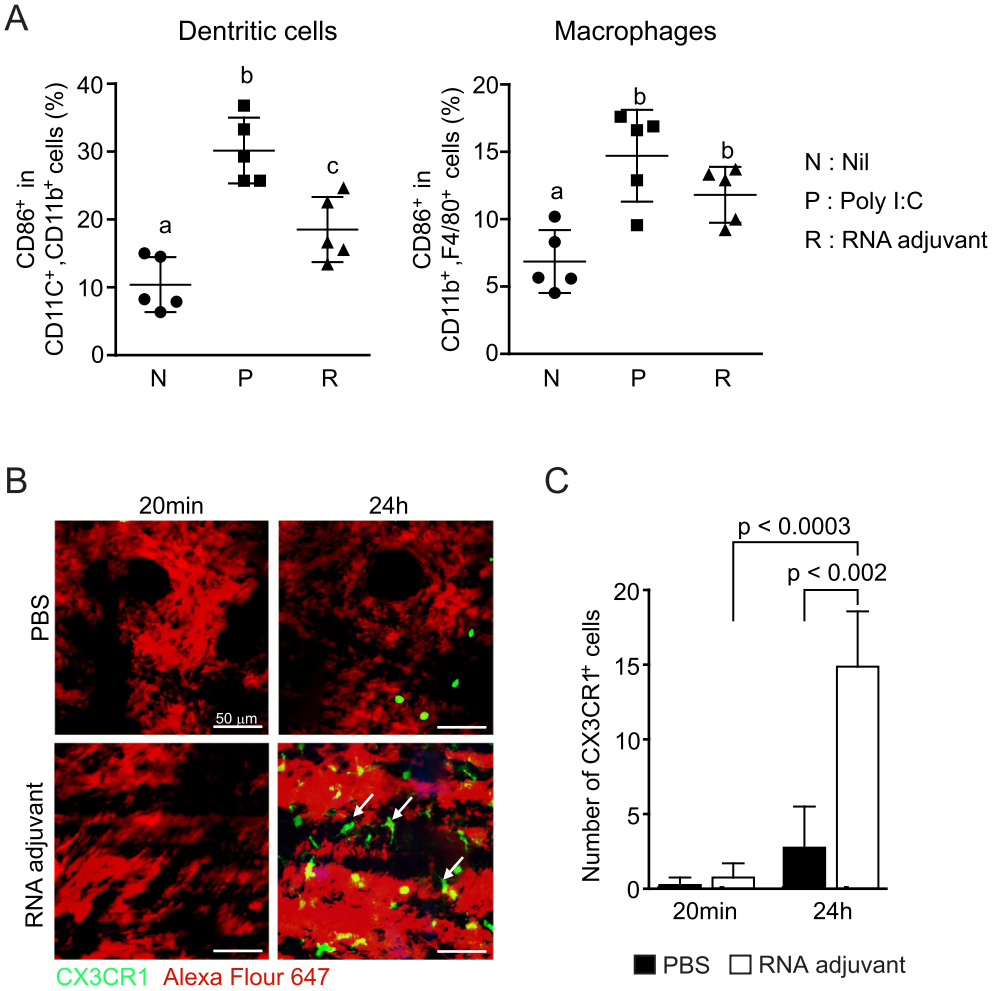

Fig. 3. The RNA adjuvant recruits DCs and macrophages to the injection site and increases their retention in the dLN at 24 h post-injection. BALB/c mice were intramuscularly injected into the quadriceps muscle, and CX3CR1-GFP mice were subcutaneously injected into the ear skin with RNA adjuvant or poly(I:C). (*A*) Activated DCs ($CD11c^+$-$CD11b^+CD86^+$) and macrophages ($CD11b^+F4/80^+Cd86^+$) in dLNs were counted by flow cytometry. The data were statistically analyzed by ANOVA. The significance of differences between groups is indicated by different letters of the alphabet. $p < 0.05$. Data represent the mean ± standard deviation ($n = 5$/group). (*B*) Infiltration of $CX3CR1^+$ cells (green; white arrows) by PBS and RNA adjuvant was monitored by *in vivo* imaging. Red color indicates Alexa Fluor 647 at injection sites, which spread to the surrounding space. (*C*) The frequency of DC infiltration into mouse ear skin. Data represent the mean ± standard deviation ($n = 10$ image sites). Data were statistically analyzed by Student's *t*-test. DC: dendritic cell, PBS: phosphate-buffered saline, dLN: draining lymph node. (For interpretation of the references to color in this figure legend, the reader is referred to the web version of this article.)

A

Group	G1	G2	G3	G4	G5
MERS S protein	-	+	+	+	+
Alum	-	-	+	-	+
RNA adjuvant	-	-	-	+	+

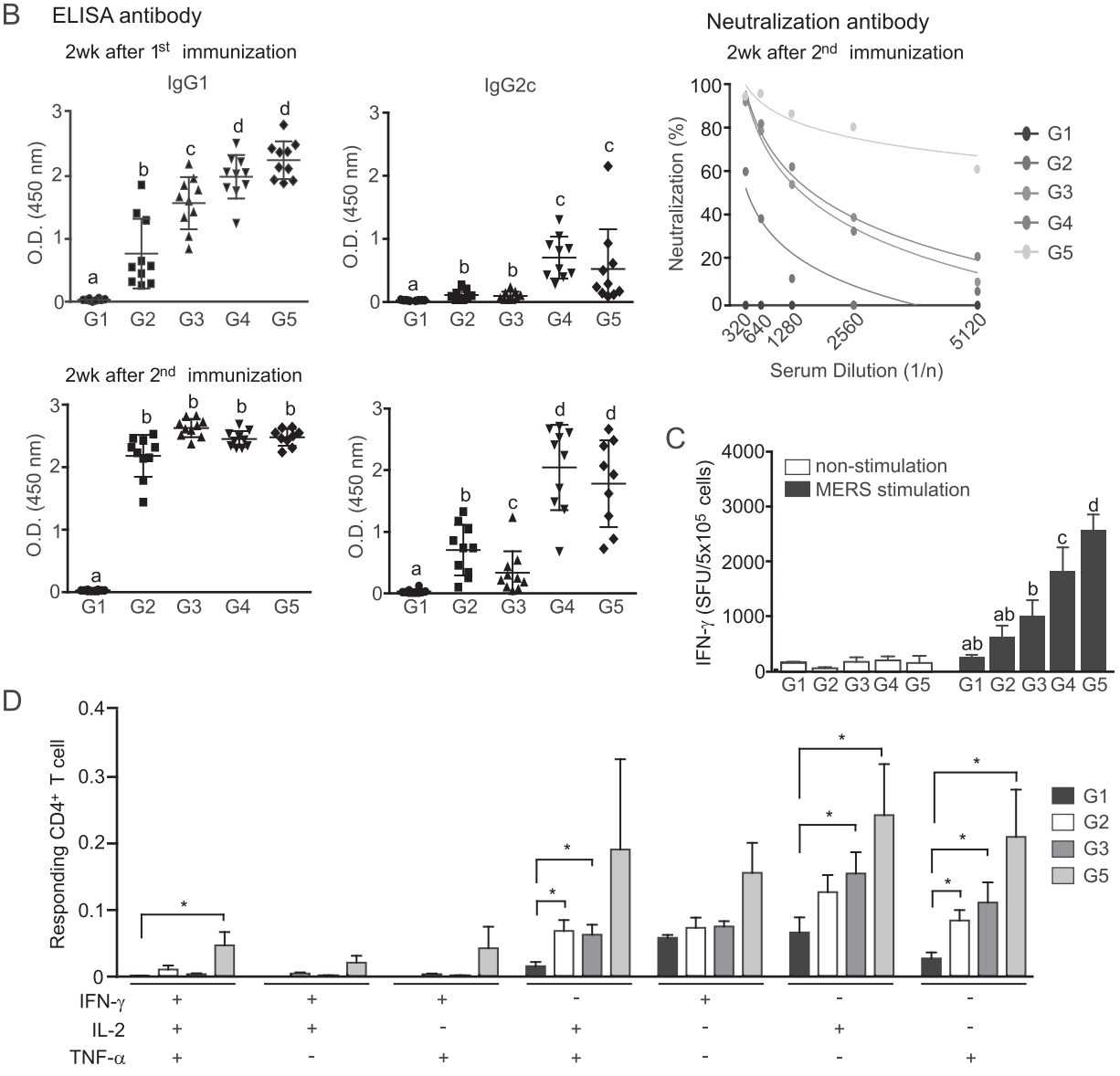

Fig. 4. RNA adjuvant formulated with MERS S soluble protein vaccine induces Th1 response, as well as an increased number of NAbs. C57BL/6 mice were intramuscularly immunized at 2-week intervals with two doses of MERS S soluble protein vaccine with/without RNA adjuvant or alum. (*A*) Overall study design. (*B*) MERS S protein-specific IgG1 and IgG2c levels measured by ELISA at 2- and 4-weeks after the first immunization. Data represent the mean ± standard deviation ($n = 10$ mice). MERS-CoV-specific NAb levels of immunized mice were determined by PRNT at 2 weeks after the second immunization. Serum from the same group was pooled ($n = 10$) and diluted 2-fold. (*C*) Splenocytes were harvested at 2 weeks after second immunization and re-stimulated for 2 days with/without the MERS S protein. The frequency of MERS S-specific IFN-γ-producing cells determined by ELISPOT. Data represent the mean ± standard deviation ($n = 3$) (triplicate results acquired in one pooled sample per group). The data were statistically analyzed by ANOVA for (B) and (C). The significance of differences between groups is indicated by different letters of the alphabet. $p < 0.05$. (*D*) Frequencies of IFN-γ, IL-2, and TNF-α-producing polyfunctional CD4 + T cells assessed by flow cytometry. Data represent the mean ± standard deviation ($n = 3$). $^{*}p < 0.05$. Data were statistically analyzed by Student's *t*-test for (D). ELISPOT: enzyme-linked immunospot, S: spike, IFN: interferon, ELISA: enzyme-linked immunosorbent assay, PRNT: plaque-reduction neutralization test, MERS: Middle East Respiratory Virus, CoV: coronavirus, NAb: neutralizing antibody.

G5 and G4 showed the highest IgG1 level (indicating a Th2 response). After boosting (at 2 weeks after second immunization), G2 to G5 showed similar IgG1 levels. Conversely, IgG2c (indicating a Th1 response) was only induced in G4 and G5 (Fig. 4B), suggesting that the RNA adjuvant induced a Th1 response. Moreover, G5 showed the highest NAb level (indicating a strong Th2 response), and G3 and G4 showed similar levels (Fig. 4B). Interestingly, G5 and G4 showed higher numbers of IFN-γ secreting cells following stimulation with the MERS S protein as compared with G2 and G3 (Fig. 4C), indicating that the RNA adjuvant induced MERS S protein-specific Th1 responses. Moreover, we observed elevations in the number of polyfunctional CD4+ T cells in G5 (Fig. 4D). These

results suggested that the RNA adjuvant promoted CD4+ T cell responses, especially Th1 responses, consequently inducing antigen-specific cellular immune responses. Furthermore, administering alum along with the RNA adjuvant generated a synergistic effect, leading to an increase in NAb levels by stimulating balanced Th1/Th2 responses.

To investigate the protective effect of immunization with the MERS S protein formulated with the RNA adjuvant plus alum (Fig. 5A), we immunized hDPP4-Tg mice, a surrogate mouse model for MERS challenge [28]. Although the body weights of G2 and G3 were immediately reduced (but quickly recovered) after challenge (Fig. 5B), we observed 100% survival (Fig. 5C), possibly due to a sufficient NAb level derived from boosting immunization, although G2 showed lower NAb levels relative to G3 in hDPP4-Tg mice (Supplementary Fig. 3).

3.5. The RNA adjuvant endows long-term immunity in VLP vaccine

To investigate the long-term immune effect of the RNA adjuvant, we immunized mice with a 10-value HPV vaccine as a VLP vaccine, an RNA adjuvant-containing 16 HPV-L1 gene (RNA adjuvant-HPV; Supplementary Fig. 1), protamine (used as a condensing component of RNA-cationic peptide complex [29]), and alum (Fig. 6A). At 2-weeks after the first immunization, the IgG1 levels of G2 and G3 were similar, whereas the IgG2a level of G3 was higher than that of G2 (Fig. 6B). After three doses (7–27 weeks after the first immunization), G2 and G3 showed similar IgG1 and IgG2a levels (Fig. 6B); however, G3 showed higher NAb levels against 11, 16, 18, 35, 45, 52, and 58 HPVs, similar levels against 6 and 33 HPVs, and lower levels against 31 HPVs than G2 (Fig. 6C). Furthermore, the frequency of IFN-γ-secreting cells among splenocytes from G3 after stimulation with 16, 18, or all HPV-L1 proteins was significantly higher than that of G2, suggesting that G3 maintained an active HPV-L1-specific Th1 response, even at 27-weeks post-immunization (Fig. 6D). This indicated that the RNA adjuvant-HPV helped maintain long-lasting humoral and cellular immune responses.

3.6. The RNA adjuvant-induced Th1 response is dependent upon both CD4+ and CD8+ T cells and TLR7

Our results indicated that the RNA adjuvant induced T cell activation and expression of TLR7-related genes, as well as a balanced Th1/Th2 response. To investigate this process, *Tlr7*-KO and WT mice were immunized with the MERS S protein, RNA adjuvant, and alum. As expected, IgG1 levels of in the KO mice were lower than those of WT mice at 2-weeks after first immunization (Fig. 7A). However, IgG1 was increased, while IgG2c was not, in KO mice at 2-weeks after second immunization (Fig. 7A), suggesting that the RNA adjuvant might have partially overcome the loss of TLR7 for Th2 induction but not Th1 via boosting. Mouse embryonic fibroblasts treated with the RNA adjuvant or a positive control (R848 as TLR7/8 agonist and poly I:C) showed the induction of Myd88, RIG-I, melanoma differentiation-associated protein 5, phosphorylated interferon regulatory factor 3, and TANK-binding kinase 1/NF-κB activating kinase, which are the downstream molecules of TLR7 and RIG-I-like receptor pathways [30] (Supplementary Fig. 4), suggesting that, while Th1 activation by RNA adjuvant may be critically dependent on the TLR7 pathway, Th2 activation by RNA adjuvant may be induced by multiple mechanisms that bypass the TLR7 signaling pathway, such as the pathway involving RIG-I-like receptor, which is one of other pattern recognition receptors (PRRs).

To investigate the necessity of CD4+, CD8+, or both T cells to activate the Th1 response, these were respectively depleted in the mouse spleen (Fig. 7B and Supplementary Fig. 5). CD4-depleted mice (G3) showed significant reductions in IgG1 and IgG2c levels, whereas CD8-depleted mice (G4) showed no reduction in IgG1 levels but had reduced IgG2c levels. Moreover, mice lacking both CD4 and CD8 (G5) showed reductions in both IgG1 and IgG2c levels (Fig. 7C), indicating that IgG1 was dependent upon CD4+ T cell activation alone, whereas IgG2c was dependent on both CD4+ and CD8+ T cell activation. Moreover, IFN-γ-secreting cells (representing the Th1 response) after treatment with mixed CD8+ T cell-epitope peptides [31] were not induced

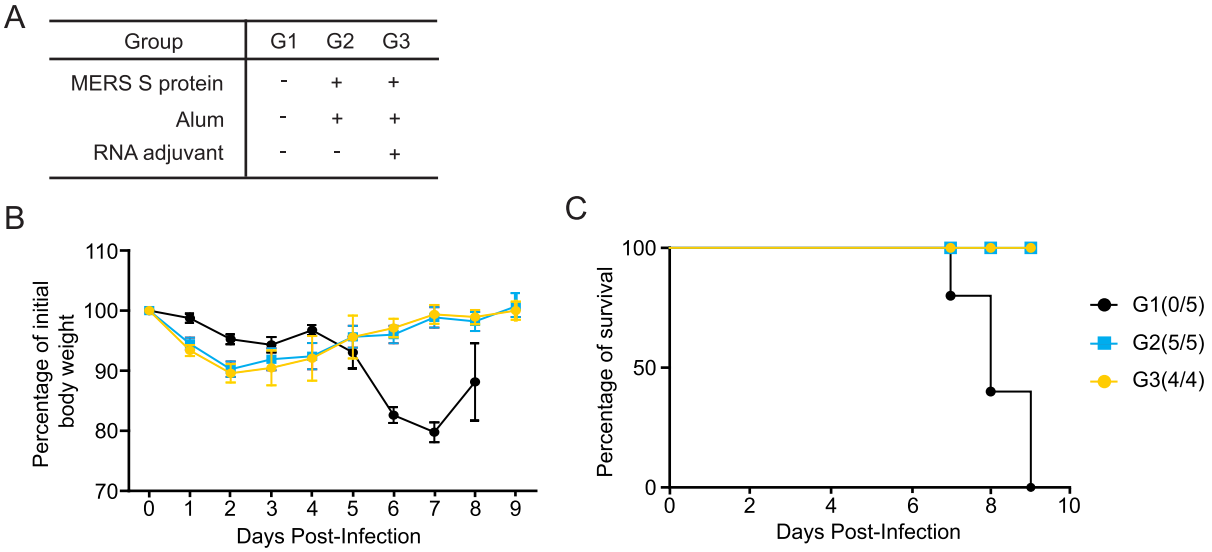

Fig. 5. Immunization with RNA adjuvant-formulated MERS S soluble protein vaccine and/or alum protects against MERS-CoV challenge. hDPP4-Tg mice were intramuscularly immunized with MERS S soluble protein vaccine with/without RNA adjuvant and/or alum. (*A*) Overall study design for hDPP4-Tg mice. (*B*) Percentage body weight and survival of hDPP4-Tg mice after challenge with 5×10^3 PFU of MERS-CoV/mouse at 3 weeks after second immunization ($n = 4$–5 mice). (*C*) Survival of hDPP4-Tg mice after challenge with MERS-CoV. (survival # / total #). Tg: transgenic, MERS: Middle East Respiratory Virus, CoV: coronavirus, Nab: neutralizing antibody, S: spike, PFU: plaque-forming unit.

A

Group	G1	G2	G3
HPV VLPs + Alum	-	+	+
RNA adjuvant-HPV	-	-	+
Carrier	-	-	P

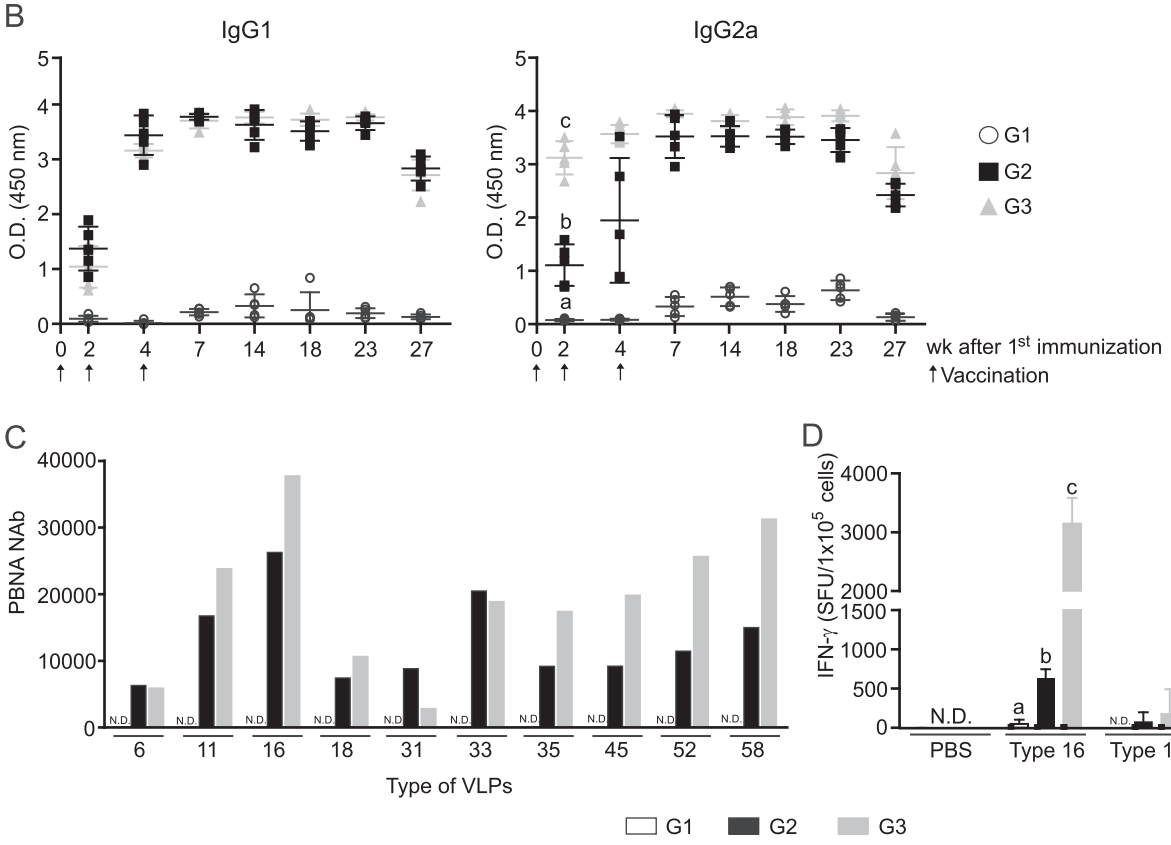

Fig. 6. RNA adjuvant-HPV-formulated VLP vaccine induces antigen-specific long-term immunity. BALB/c mice were intramuscularly immunized at 2-week intervals with three doses of 10-value VLP-HPV-L1 with alum and with/without protamine-formulated RNA adjuvant-HPV. (*A*) Overall study design. (*B*) HPV-L1-specific IgG1 and IgG2a levels were measured by ELISA from 2-weeks to 27-weeks after the first immunization. Data represent the mean ± standard deviation ($n = 5$ mice). (*C*) HPV-L1 NAb levels against different types of VLPs in the immunized mice were determined by pseudovirus PRNT at 27 weeks after the first immunization. Serum from the same group ($n = 5$) was pooled. (*D*) Splenocytes were harvested at 27 weeks after the first immunization and re-stimulated for 2 days with/without type 16 or 18 HPV-L1 protein or 10 types of VLP-HPV-L1. The frequency of HPV-specific IFN-γ-producing cells was determined by ELISPOT. Data represent the mean ± standard deviation ($n = 3$) (triplicate results acquired from one pooled sample per group). The data were statistically analyzed by ANOVA for (B) and (D). The significance of differences between groups is indicated by different letters of the alphabet. $p < 0.05$. ELISPOT: enzyme-linked immunospot, IFN: interferon, VLP: virus-like particle, HPV: human papillomavirus, ELISA: enzyme-linked immunosorbent assay, PRNT: plaque-reduction neutralization test, NAb: neutralizing antibody.

in G4 and G5 (Fig. 7D). These data showed that the RNA adjuvant enhanced an antigen-specific Th1 response via the TLR7 signaling pathway and CD4+/CD8+ T cell activation.

4. Discussion

In this study, we demonstrated the adjuvant effect of CrPV-IGR IRES-derived ssRNA [23] using protein-based vaccines. The RNA adjuvant induced the expression of genes related to the innate immune response (IFN and TLR-Myd88), T cell activation, and leukocyte chemotaxis similar to poly(I:C) in hPBMCs; however, the induction levels were lower than those by poly(I:C), and most genes returned to normal levels within 24 h (Fig. 1). This transient induction of genes by the RNA adjuvant may be evidence of vaccine safety. Similarly, a previous report demonstrated the rapid disappearance of the RNA platform within 24 h after injection [23]. We did not observe any adverse effects, such as autoimmune symptoms, changes in liver function, or organ damage, in the RNA adjuvant-immunized mice, even at a higher dose (200 μg/-mouse) (data not shown). Although poly(I:C) can be a superior adjuvant, safety concerns, such as an excessive immune response, represents a significant drawback [15]. However, our RNA adjuvant appeared to overcome this safety issue without decreasing the immune-stimulation effect.

Among the key factors induced in RNA adjuvant-treated hPBMCs, intercellular adhesion molecule-1, IL-6, IL-15, CD80, and STAT1/3 were induced (Fig. 1). In particular, IL-6, which is highly expressed in CD4+ T cells, is partially responsible for Th2 cytokine production in Th1-differentiated cells via protein kinase C theta and NF-κB signaling pathways [32]. Additionally, IL-15 stimulates T and natural killer cell immunity and promotes the generation of long-lived memory T cells [33]. Furthermore, STAT1 functions as a central regulator of innate and adaptive immunity, and STAT3 is essential for DC, Tfh cell, and memory CD8+ T cell development [34,35]. Given that the RNA adjuvant activated the Th1 response and induced long-term immunity (Figs. 4–6), induction of these genes might have played an important role in this immune response.

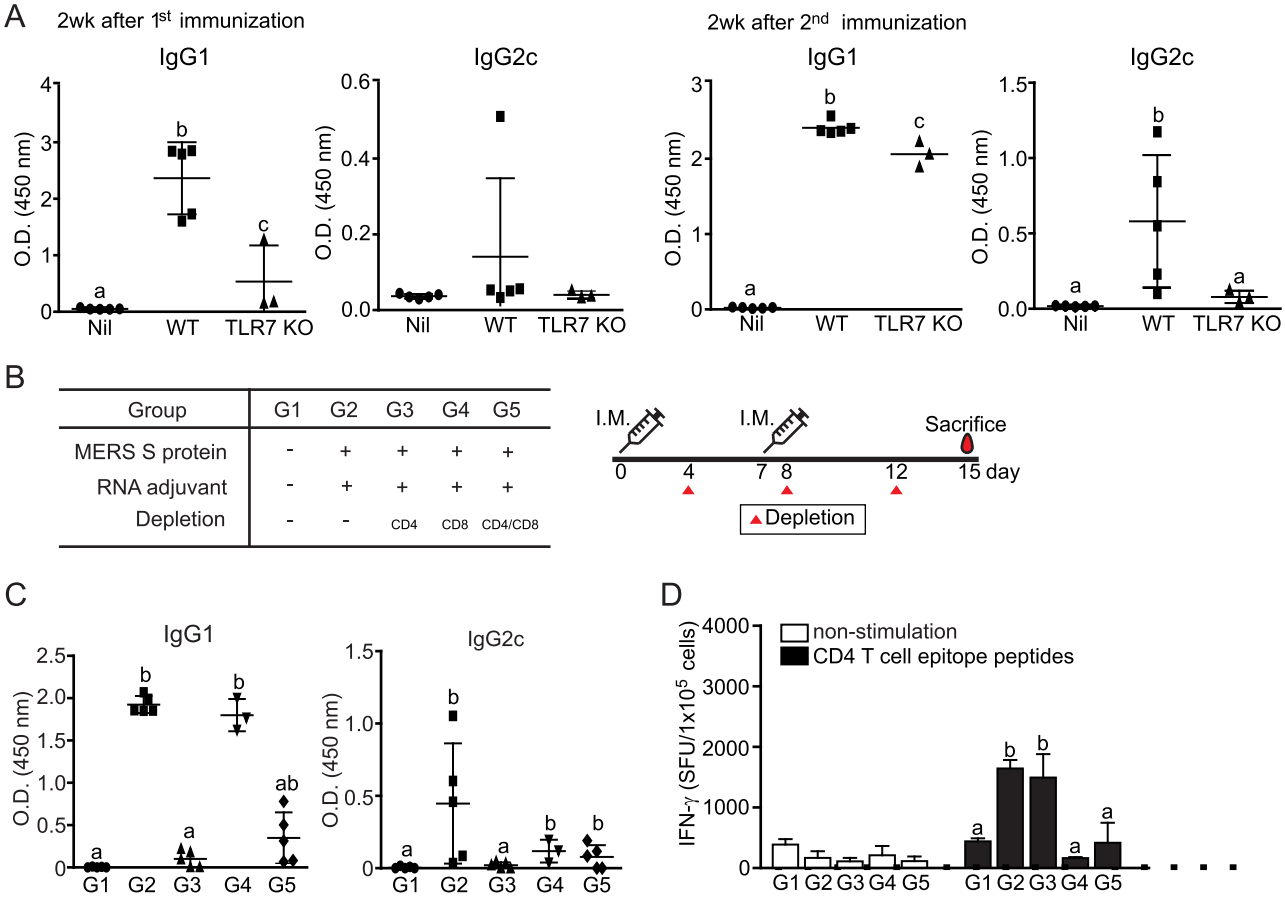

Fig. 7. The RNA adjuvant induces a Th1 response through TLR7 and CD4+/CD8+ T cells. *Tlr7*-KO mice and C57BL/6 (WT) mice were intramuscularly immunized at 2-week intervals with two doses of 1 μg MERS S soluble protein vaccine, 20 μg formulated RNA adjuvant or alum. (*A*) MERS S protein-specific IgG1 and IgG2c levels were measured by ELISA at 2 weeks after the first and second immunizations. Data represent the mean ± standard deviation (n = 3–5 mice). (*B*) Overall study design and mouse schedule for immunization and anti-CD4 or CD8 treatment. (*C*) MERS S protein-specific IgG1 and IgG2c levels were measured by ELISA at 2 weeks after the second immunization. Data represent the mean ± standard deviation (n = 3–5 mice). (*D*) The frequency of MERS S protein-specific IFN-γ-producing cells was determined by ELISPOT after treatment with a CD8+ T cell-epitope peptide mixture (7 peptides for C57BL/6, as described previously [30]) or MERS S protein. Data represent the mean ± standard deviation (n = 3) (triplicate results acquired from one pooled sample per group). The data were statistically analyzed by ANOVA for (A), (C), and (D). The significance of differences between groups is indicated by different letters of the alphabet. $p < 0.05$. Th: T helper cell, ELISPOT: enzyme-linked immunospot, S: spike, IFN: interferon, ELISA: enzyme-linked immunosorbent assay, PRNT: plaque-reduction neutralization test, MERS: Middle East Respiratory Virus, TLR: Toll-like receptor, KO: knockout, WT: wild-type.

Interestingly, we found that the expression of genes associated with the innate immune response, especially type 1 IFN-related genes, was similar between the RNA adjuvant-treated hPBMCs and PBMCs from a live-attenuated YF17D-immunized patient (Fig. 2). Moreover, it is also important that *IRF7* expression was induced in RNA adjuvant-treated hPBMCs similar to that observed following immunization with YF17D because IRF7 is an essential molecule for antigen-specific IFN production promoting T and B cell activation [36]. These data assumed that the RNA adjuvant may make inactivated and protein-based vaccines function like a live attenuated vaccine. However, further studies are required to confirm this hypothesis.

Furthermore, *Tlr7*-KO mice and CD4+/CD8+ T cell-depleted mice did not show any RNA adjuvant effects (Fig. 7), consistent with previous results [22,37,38]. These data indicated that this RNA adjuvant might be efficacious for inducing a broad immune response mediated through TLR7 signaling and T cell activation. However, the PRR for the RNA adjuvant cannot be confined to TLR7 alone, as the RNA adjuvant could induce RIG-I-like receptor pathway-related molecules similar to R848 and poly I:C (Supplementary Fig. 4). This indicated that the RNA adjuvant is recognized by RIG-I-like receptor in addition to TLR7 to activate an immune response. These data are accordance with a previous study, which showed that RNA based adjuvants triggered TLR- and RIG-I-like helicase-dependent effect [22]. Therefore, the boosting with RNA adjuvant may partially induce an IgG1 (Th2) response in *Tlr7*-KO mice through the RIG-I-like pathway. However, we do not know why this pathway cannot induce IgG2c (Th1). Further studies are required to understand the detailed underlying mechanism.

In addition, although the RNA adjuvant mediated its effects through the TLR7 signaling pathway, we did not use TLR agonists, such as imiquimod (TLR7 agonist) and resiquimod (TLR7/8 agonist), which are chemical adjuvants [39], as a controls in this study, as this study focused on RNA-based adjuvants, such as poly I:C, but not chemical agonist-adjuvants. Poly I:C is a dsRNA that shows strong adjuvanticity in inactivated and protein-based vaccines [12–14]; therefore, it was used as a control in this study.

Upon immunization with the MERS S protein vaccine together with alum and the RNA adjuvant, MERS S-specific NAb production increased synergistically (Fig. 4B). Our data suggest that T cell activation of G5 may also show a synergistic increase, however, more data are needed to confirm this (Fig. 4D). Additionally, given the strong immune-stimulating effect of the RNA adjuvant, it was unsurprising that the RNA adjuvant-HPV group was able to maintain HPV-specific NAb levels and the Th1 response, even at 27-weeks after first immunization (Fig. 6). These results indicated that the RNA adjuvant triggered long-term immunity, including humoral and cellular immune responses. This is an important fea-

ture, given that HPV should have a long-term protective effect after vaccination.

Here, we used one RNA molecule derived from the CrPV-IGR IRES in the absence of target genes as the adjuvant and demonstrated its adjuvanticity for the MERS S protein vaccine. The RNA adjuvant-containing target gene HPV-L1 also showed an immune-stimulating effect. Therefore, although we previously showed that an RNA platform could express a coding gene [23], RNA adjuvant including target gene is not critical to ensure adjuvanticity. However, should this RNA platform be used as an RNA vaccine, it needs to encode target genes. Further, improvements in the delivery strategy to increase the expression efficiency in the inoculated animal muscle are warranted. Interestingly, we compared the adjuvanticity of CrPV-IGR IRES-derived RNA with those of other RNA virus-derived adjuvants, including coxsackievirus B3 (CVB3) and encephalomyocarditis virus (EMCV) IRESs-derived RNAs. CrPV and CVB3 IRES-derived RNAs showed higher adjuvant effects compared to that of the EMCV IRES-derived RNA (data not shown). Studies are underway on the effect of the viral IRES type on the immune effect.

5. Conclusion

Use of the RNA adjuvant as an immune stimulator, regardless of the presence of antigen-encoding genes, has many advantages, including its applicability for protein-based vaccines, simple manufacturing procedures, and easy standardization. Moreover, it can potentially overcome challenges associated with protein-subunit vaccines, such as weak T cell activation. The associated immune responses consequently promote high NAb levels and balanced Th1 and Th2 responses, resulting in long-term immunity. Therefore, since the RNA adjuvant exhibited immune-enhancing capacity, it might be valuable not only as a first-line vaccine in an epidemic emergency but also to improve protein-based vaccine efficacy.

Declaration of Competing Interest

The authors declare that they have no known competing financial interests or personal relationships that could have appeared to influence the work reported in this paper.

Acknowledgments

The authors thank Drs Jung Joo Hong and Hanseul Oh for technical assistance, Hae-Yung Ahn for assistance with animal care, and Dr. Jin-Seul Kim for assistance with HPV vaccine.

Financial support

J.-H. Nam was supported by the Korean Health Technology R&D Project through the Korea Health Industry Development Institute (KHIDI) funded by the Ministry of Health & Welfare, Republic of Korea (HI15C2955), the Basic Science Research Program through the NRF funded by the Ministry of Science, ICT & Future Planning (NRF-2015M3A9B5030157), and the Catholic University of Korea, Research Fund 2018. M. Song was supported by the Ministry of Health & Welfare, Republic of Korea (HI15C2971).

Author contributions

J.-H. Nam and H.-J. Park designed all studies. J.-H. Nam and S.-M. Lee analyzed the results. S.-M. Lee, K.W. Kang, and S.R. Ryu measured MERS NAb levels and challenged with MERS-CoV. H.W. Kwak, H.-J. Park, H.L. Ko, H.-J. Kim, and R.-H. Kim did the MERS, and the HPV related experiments. M.H. Cha and H.W. Kwak analyzed the RNA-seq data. J.O. Kim, M. Song, D.G. Jeong, and H. Kim supplied the vaccines, the vaccine candidates, and hDPP4-Tg mice. E.-C. Shin did the polyfunctional T cell assay. J.-H. Nam and H. Park wrote the manuscript with help from the coauthors.

Conflicts of interest

There are no conflicts of interests to declare.

Appendix A. Supplementary material

Supplementary data to this article can be found online at https://doi.org/10.1016/j.vaccine.2019.07.070.

References

[1] Smith J, Lipsitch M, Almond JW. Vaccine production, distribution, access, and uptake. Lancet 2011;378:428–38. https://doi.org/10.1016/S0140-6736(11)60478-.
[2] Christensen D. Vaccine adjuvants: why and how? Hum Vaccin Immunother 2016;12:2709–11. https://doi.org/10.1080/21645515.2016.1219003.
[3] Minor PD. Live attenuated vaccines: historical successes and current challenges. Virology 2015;479–480:379–92. https://doi.org/10.1016/j.virol.2015.03.032.
[4] Del Giudice G, Rappuoli R, Didierlaurent AM. Correlates of adjuvanticity: a review on adjuvants in licensed vaccines. Semin Immunol 2018;39:14–21. https://doi.org/10.1016/j.smim.2018.05.001.
[5] Awate S, Babiuk LA, Mutwiri G. Mechanisms of action of adjuvants. Front Immunol 2013;4:114. https://doi.org/10.3389/fimmu.2013.00114.
[6] Moyer TJ, Zmolek AC, Irvine DJ. Beyond antigens and adjuvants: formulating future vaccines. J Clin Invest 2016;126:799–808. https://doi.org/10.1172/JCI81083.
[7] Marrack P, McKee AS, Munks MW. Towards an understanding of the adjuvant action of aluminium. Nat Rev Immunol 2009;9:287–93. https://doi.org/10.1038/nri2510.
[8] McKee AS, Marrack P. Old and new adjuvants. Curr Opin Immunol 2017;47:44–51. https://doi.org/10.1016/j.coi.2017.06.005.
[9] He P, Zou Y, Hu Z. Advances in aluminum hydroxide-based adjuvant research and its mechanism. Hum Vaccin Immunother 2015;11:477–88. https://doi.org/10.1080/21645515.2014.100402.
[10] Duthie MS, Windish HP, Fox CB, Reed SG. Use of defined TLR ligands as adjuvants within human vaccines. Immunol Rev 2011;239:178–96. https://doi.org/10.1111/j.1600-065X.2010.00978.x.
[11] Bracci L, La Sorsa V, Belardelli F, Proietti E. Type I interferons as vaccine adjuvants against infectious diseases and cancer. Expert Rev Vacc 2008;7:373–81. https://doi.org/10.1586/14760584.7.3.373.
[12] Singh B, Postic B. Enhanced resistance of mice to virulent Japanese B encephalitis virus following inactivated vaccine and poly(I:C). J Infect Dis 1970;122:339–42.
[13] Martins KA, Bavari S, Salazar AM. Vaccine adjuvant uses of poly-IC and derivatives. Expert Rev Vacc 2015;14:447–59. https://doi.org/10.1586/14760584.2015.966085.
[14] Caskey M, Lefebvre F, Filali-Mouhim A, Cameron MJ, Goulet JP, Haddad EK, et al. Synthetic double-stranded RNA induces innate immune responses similar to a live viral vaccine in humans. J Exp Med 2011;208:2357–66. https://doi.org/10.1084/jem.20111171.
[15] Hafner AM, Corthésy B, Merkle HP. Particulate formulations for the delivery of poly(I:C) as vaccine adjuvant. Adv Drug Deliv Rev 2013;65:1386–99. https://doi.org/10.1016/j.addr.2013.05.013.
[16] Crow MK. Type I interferon in the pathogenesis of lupus. J Immunol 2014;192:5459–68.
[17] Antonelli LR, Rothfuchs AG, Gonçalves R, Roffê E, Cheever AW, Bafica A, et al. Intranasal Poly-IC treatment exacerbates tuberculosis in mice through the pulmonary recruitment of a pathogen-permissive monocyte/macrophage population. J Clin Invest 2010;120:1674–82. https://doi.org/10.1172/JCI40817.
[18] Steinhagen F, Kinjo T, Bode C, Klinman DM. TLR-based immune adjuvants. Vaccine 2011;29:3341–55. https://doi.org/10.1016/j.vaccine.2010.08.002.
[19] Martinez-Gil L, Goff PH, Hai R, Garcia-Sastre A, Shaw ML, Palese P. A Sendai virus-derived RNA agonist of RIG-I as a virus vaccine adjuvant. J Virol 2013;87:1290–300. https://doi.org/10.1128/JVI.02338-12.
[20] Pardi N, Hogan MJ, Naradikian MS, Parkhouse K, Cain DW, Jones L, et al. Nucleoside-modified mRNA vaccines induce potent T follicular helper and germinal center B cell responses. J Exp Med 2018;215:1571–88. https://doi.org/10.1084/jem.20171450.
[21] Fotin-Mleczek M, Duchardt KM, Lorenz C, Pfeiffer R, Ojkic-Zrna S, Probst J, et al. Messenger RNA-based vaccines with dual activity induce balanced TLR-7 dependent adaptive immune responses and provide antitumor activity. J Immunother 2011;34:1–15. https://doi.org/10.1097/CJI.0b013e3181f7dbe8.

[22] Ziegler A, Soldner C, Lienenklaus S, Spanier J, Trittel S, Riese P, et al. A new RNA-based adjuvant enhances virus-specific vaccine responses by locally triggering TLR- and RLH-dependent effects. J Immunol 2017;198:1595–605.
[23] Ko HL, Park HJ, Kim J, Kim H, Youn H, Nam JH. Development of an RNA expression platform controlled by viral internal ribosome entry sites. J Microbiol Biotechnol 2019;29:127–40. https://doi.org/10.4014/jmb.1811.11019.
[24] Wang JW, Jagu S, Wang C, Kitchener HC, Daayana S, Stern PL, et al. Measurement of neutralizing serum antibodies of patients vaccinated with human papillomavirus L1 or L2-based immunogens using furin-cleaved HPV Pseudovirions. PLoS ONE 2014;9:. https://doi.org/10.1371/journal.pone.0101576e101576.
[25] Barba-Spaeth G, Longman RS, Albert ML, Rice CM. Live attenuated yellow fever 17D infects human DCs and allows for presentation of endogenous and recombinant T cell epitopes. J Exp Med 2005;202:1179–84. https://doi.org/10.1084/jem.20051352.
[26] Gaucher D, Therrien R, Kettaf N, Angermann BR, Boucher G, Filali-Mouhim A, et al. Yellow fever vaccine induces integrated multilineage and polyfunctional immune responses. J Exp Med 2008;205:3119–31. https://doi.org/10.1084/jem.20082292.
[27] Querec TD, Akondy RS, Lee EK, Cao W, Nakaya HI, Teuwen D, et al. Systems biology approach predicts immunogenicity of the yellow fever vaccine in humans. Nat Immunol 2009;10:116–25. https://doi.org/10.1038/ni.1688.
[28] Agrawal AS, Garron T, Tao X, Peng BH, Wakamiya M, Chan TS, et al. Generation of a transgenic mouse model of Middle East respiratory syndrome coronavirus infection and disease. J Virol 2015;89:3659–70. https://doi.org/10.1128/JVI.03427-14.
[29] Shukla RS, Qin B, Cheng K. Peptides used in the delivery of small noncoding RNA. Mol Pharm 2014;11:3395–408. https://doi.org/10.1021/mp500426r.
[30] Chow KT, Gale Jr M, Loo YM. RIG-I and other RNA sensors in antiviral immunity. Annu Rev Immunol 2018;36:667–94. https://doi.org/10.1146/annurev-immunol-042617-053309.
[31] Zhao J, Li K, Wohlford-Lenane C, Agnihothram SS, Fett C, Zhao J, et al. Rapid generation of a mouse model for Middle East respiratory syndrome. Proc Natl Acad Sci USA 2014;111:4970–5. https://doi.org/10.1073/pnas.1323279111.
[32] Sofi MH, Li W, Kaplan MH, Chang CH. Elevated IL-6 expression in CD4 T cells via PKCtheta and NF-kappaB induces Th2 cytokine production. Mol Immunol 2009;46:1443–50. https://doi.org/10.1016/j.molimm.2008.12.014.
[33] Pilipow K, Roederer M, Waldmann TA, Mavilio D, Lugli E. IL15 and T-cell stemness in T-cell-based cancer immunotherapy. Cancer Res 2015;75:5187–93. https://doi.org/10.1158/0008-5472.CAN-15-1498.
[34] Decker T, Stockinger S, Karaghiosoff M, Müller M, Kovarik P. IFNs and STATs in innate immunity to microorganisms. J Clin Invest 2002;109:1271–7. https://doi.org/10.1172/JCI15770.
[35] Hillmer EJ, Zhang H, Li HS, Watowich SS. STAT3 signaling in immunity. Cyto Growth Factor Rev 2016;31:1–15.
[36] Suschak JJ, Wang S, Fitzgerald KA, Lu S. A cGAS-independent STING/IRF7 pathway mediates the immunogenicity of DNA vaccines. J Immunol 2016;196:310–6. https://doi.org/10.4049/jimmunol.1501836.
[37] Fierer J, Waters C, Walls L. Both CD4+ and CD8+ T cells can mediate vaccine-induced protection against Coccidioides immitis infection in mice. J Infect Dis 2006;19:1323–31. https://doi.org/10.1086/502972.
[38] Provine NM, Badamchi-Zadeh A, Bricault CA, Penaloza-MacMaster P, Larocca RA, Borducchi EN, et al. Transient CD4+ T cell depletion results in delayed development of functional vaccine-elicited antibody responses. J Virol 2016;90:4278–88. https://doi.org/10.1128/JVI.00039-16.
[39] Smits EL, Ponsaerts P, Berneman ZN, Van Tendeloo VF. The use of TLR7 and TLR8 ligands for the enhancement of cancer immunotherapy. Oncologist 2008;13:859–75. https://doi.org/10.1634/theoncologist.2008-0097.